



**INTERNATIONAL JOURNAL OF ENGINEERING SCIENCES & RESEARCH
TECHNOLOGY**

A Proportional Analysis of Image Fusion Methods

Sanjaykumar Bhalchandra Dixit^{*1}, Rahul Keru Patil²

^{*1,2}Assistant Professor, College of Engineering, Malegaon(Bk), India
dixit_sanjay75@rediffmail.com

Abstract

The fusion of high-spectral/low-spatial resolution multi-spectral and low-spectral high-spatial resolution panchromatic satellite images is a very useful technique in various applications of remote sensing. Recently, some studies showed that a wavelet-based image fusion method provides high quality spectral content in fused images. However, most wavelet-based methods yield fused results with spatial resolution that is less than that obtained via the Brovey, IHS, and PCA fusion methods. In this paper, we introduce a new method based on a curvelet transform, which represents edges better than wavelets. Since edges play a fundamental role in image representation, one effective means to enhance spatial resolution is to enhance the edges. The curvelet-based image fusion method provides richer information in the spatial and spectral domains simultaneously. We performed Landsat ETM+ image fusion and found that the proposed method provides optimum fusion results.

Keywords: Image Fusion, Multiresolution analysis, Landsat ETM+ image, Wavelet transform, Curvelet transform.

Introduction

IN MANY remote sensing and mapping applications, the fusion of multispectral and panchromatic images is a very important issue. In this regard, in the field of satellite image classification, the quality of the image classifier is affected by the fused image's quality. To date, many image fusion techniques and software tools have been developed. The well-known methods include the Brovey, the IHS (Intensity, Hue, Saturation) colour model, the PCA (Principal Components Analysis) method, and the wavelet based method [1]. Assessment of the quality of fused images is another important issue. proposed an approach utilizing criteria that can be employed in the evaluation of the spectral quality of fused satellite images [2].

If the objective of image fusion is to construct synthetic images that are closer to reality, then the Brovey, IHS, and PCA fusion methods are satisfactory [1]. However, one limitation of these methods is some distortion of spectral characteristics in the original multispectral images. Recently, developments in wavelet analysis have provided a potential solution to this is developed an approach to fuse a high-resolution panchromatic image with a low-resolution multispectral image based on wavelet decomposition [3]. the ARSIS concept for fusing high spatial and spectral resolution images based on a multiresolution analysis of a two-band wavelet transformation.

The wavelet-based image fusion method provides high spectral quality in fused satellite

images. However, fused images by wavelets have much less spatial information than those by the Brovey, IHS, and PCA methods. In many remote sensing applications, the spatial information of a fused image is as an important factor as the spectral information. In other words, it is necessary to develop an advanced image fusion method so that fused images have the same spectral resolution as multispectral images and the same spatial resolution as a panchromatic image with minimal artifacts.

Recently, other multi-scale systems have been developed, including ridgelets and curvelets [4]–[6]. These approaches are very different from wavelet-like systems. Curvelets and ridgelets take the form of basic elements, which exhibit very high directional sensitivity and are highly anisotropic. Therefore, the curvelet transform represents edges better than wavelets, and is well-suited for multiscale edge enhancement [6].

In this paper, we introduce a new image fusion method based on a curvelet transform. The fused image using the curvelet-based image fusion method yields almost the same detail as the original panchromatic image, because curvelets represent edges better than wavelets. It also gives the same colour as the original multispectral images, because we use the wavelet-based image fusion method in our algorithm. As such, this new method is an optimum method for image fusion. in this study we develop a new approach for fusing lansat ETM+ panchromatic

and multispectral images based on the curvelet transform.

The remainder of this paper is organized as follows. The next section describes the theoretical basis of the ridgelets and curvelets. A new image fusion approach for Lansat ETM+ panchromatic and multispectral images based on the curvelet transform is subsequently presented.

This is followed by a discussion of the image fusing experiments. Next, the experimental results are analysed. Finally, the proposed method is compared with previous methods developed for image fusion, including the wavelet method and the IHS method.

IHS METHOD

This method is based on the transformation of RGB multispectral channels into HIS (Hue-Intensity-Saturation). The Intensity component is the most important component. In this method, we substitute the Intensity component by the panchromatic image and then the inverse transformation (HIS to RGB) is done.

The IHS fusion for each pixel can be formulated by the following procedure:

Step 1)

$$\begin{bmatrix} I \\ v_1 \\ v_2 \end{bmatrix} = \begin{bmatrix} \frac{1}{3} & \frac{1}{3} & \frac{1}{3} \\ -\frac{\sqrt{2}}{6} & -\frac{\sqrt{2}}{6} & \frac{2\sqrt{2}}{6} \\ \frac{1}{\sqrt{2}} & \frac{-1}{\sqrt{2}} & 0 \end{bmatrix} \begin{bmatrix} R \\ G \\ B \end{bmatrix}$$

Step 2) The intensity component I is replaced by the Pan image.

Step 3)

$$\begin{bmatrix} F(R) \\ F(G) \\ F(B) \end{bmatrix} = \begin{bmatrix} 1 & -\frac{1}{\sqrt{2}} & \frac{1}{\sqrt{2}} \\ 1 & \frac{1}{\sqrt{2}} & \frac{1}{\sqrt{2}} \\ 1 & \sqrt{2} & 0 \end{bmatrix} \begin{bmatrix} Pan \\ v_1 \\ v_2 \end{bmatrix} = \begin{bmatrix} 1 & -\frac{1}{\sqrt{2}} & \frac{1}{\sqrt{2}} \\ 1 & \frac{1}{\sqrt{2}} & \frac{1}{\sqrt{2}} \\ 1 & \sqrt{2} & 0 \end{bmatrix} \begin{bmatrix} I + (Pan - I) \\ v_1 \\ v_2 \end{bmatrix} = \begin{bmatrix} R + (Pan - I) \\ G + (Pan - I) \\ B + (Pan - I) \end{bmatrix}$$

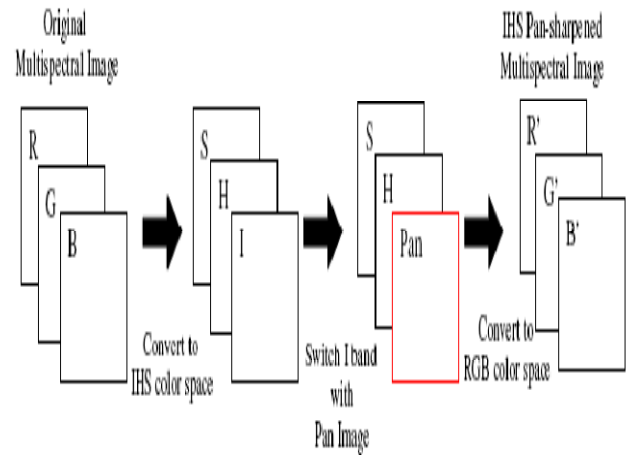


Fig.1 Original multispectral image to IHS Pan-sharpened multispectral image.

Wavelet transform Method

The most common form of transform image fusion is real valued wavelet transform fusion [1, 2, 3, 4]. As with all transform fusion techniques, all the input images are transformed and combined in the transform domain before an inverse transform results in the resultant fused image. The combination of the transformed images is achieved using a defined fusion rule. This rule can be as simple as choosing to retain the largest coefficient or more complicated windowed coefficient checks (see section 6).

Wavelet Transform in Image Fusion

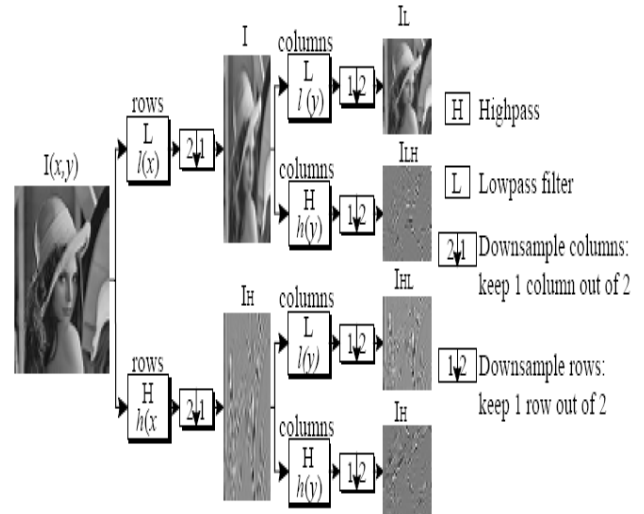


Fig. 1. DWT image decomposition

The fusion of two images within the wavelet transform domain can be formally defined considering the wavelet transforms ω of two registered input images $I1(x, y)$ and $I2(x, y)$ together with the fusion rule θ . Then, the inverse wavelet

transform ω^{-1} is computed, and the fused image $I(x, y)$ is reconstructed:

$$I(x, y) = \omega^{-1}(\theta(\omega(I_1(x, y)), \omega(I_2(x, y)))) \quad (1)$$

This process is depicted in figure 2 1

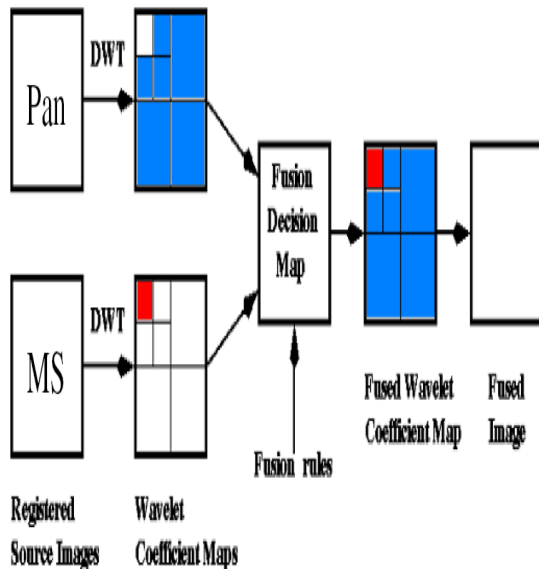


Fig. 2. Fusion of the wavelet transforms of two images.

Discrete Ridgelet Transform (DRT)

A basic strategy for calculating the continuous ridgelet transform is first to compute the Radon transform $Rf(\theta, t)$ and second to apply a one-dimensional wavelet transform to the slices $Rf(\theta, \cdot)$. A fundamental fact about the Radon transform is the projection slice formula (Deans, 1983):

$$f(\cos \theta, \sin \theta) \int Rf(\theta, t) e^{-2\pi i w t} dt \quad (10)$$

This says that the Radon transform can be obtained by applying the one-dimensional inverse Fourier transform to the two-dimensional Fourier transform restricted to radial lines through the origin. This of course suggests that approximate Radon transforms for digital data can be based on discrete fast Fourier transforms. In outline, one simply does the following,

1. 2D-FFT

Compute the two-dimensional Fast Fourier Transform (FFT) of f .

2. Cartesian to polar conversion

Using an interpolation scheme, substitute the sampled values of the Fourier transform obtained on the square lattice with sampled values of \hat{f} on a polar lattice: that is, on a lattice where the points fall on lines through the origin.

3. 1D-IFFT

Compute the one-dimensional Inverse Fast Fourier Transform (IFFT) on each line; i.e., for each value of the angular parameter.

The use of this strategy in connection with ridgelet transform has been discussed in the articles (Deans, 1983; Donoho, 1998). 3.

Digital Curvelet Transform

The idea of curvelets (Candes et al, 1999; Starck et al, 2002; Starck et al, 2003) is to represent a curve as a superposition of functions of various lengths and widths obeying the scaling law width \gg length². This can be done by first decomposing the image into subbands, i.e., separating the object into a series of disjoint scales. Each scale is then analysed by means of a local ridgelet transform.

Curvelets are based on multiscale ridgelets combined with a spatial bandpass filtering operation to isolate different scales.

This spatial bandpass filter nearly kills all multiscale ridgelets which are not in the frequency range of the filter. In other words, a curvelet is a multiscale ridgelet which lives in a prescribed frequency band. The bandpass is set so that the curvelet length and width at fine scales are related by a scaling law width \gg length² and so the anisotropy increases with decreasing scale like a power law. There is very special relationship between the depth of the multiscale pyramid and the index of the dyadic subbands; the side length of the localizing windows is doubled at every other dyadic subband, hence maintaining the fundamental property of the curvelet transform which says that elements of length about $2^{j/2}$ serve for the analysis and synthesis of the j th subband $[2^j, 2^{j+2}]$. While multiscale ridgelets have arbitrary dyadic length and arbitrary dyadic widths, curvelets have a scaling obeying width \gg length². Loosely speaking, the curvelet dictionary is a subset of the multiscale ridgelet dictionary, but which allows reconstruction.

The discrete curvelet transform of a continuum function $f(x_1, x_2)$ makes use of a dyadic sequence of scales, and a bank of filters $(P_0 f, \Delta_1 f, \Delta_2 f, \dots)$ with the property that the passband filter Δ_s is concentrated near the frequencies

$$[2^{2s}, 2^{2s+2}] s^+, \text{ e.g.,}$$

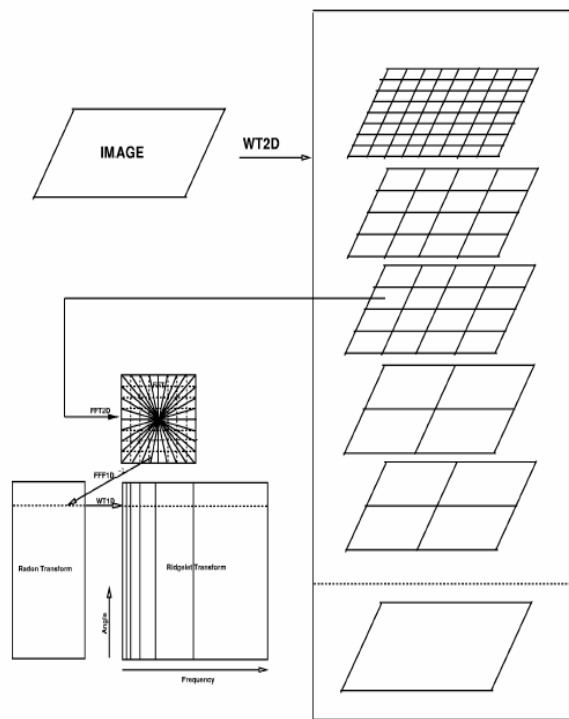


Figure 3. Curvelet transform flowgraph. The figure illustrates the decomposition of the original image into subbands followed by the spatial partitioning of each subband (i.e., each subband is decomposed into blocks). The ridgelet transform is then applied to each block .

Curvelet Transform Algorithm

In developing a transform for digital n by n data which is analogous to the discrete curvelet transform of a continuous function $f(x_1, x_2)$, we have to replace each of the continuum concepts with the appropriate digital concept mentioned in section above. Recently, Starck et al.(2002) showed that “a trous” subband filtering algorithm is especially well-adapted to the needs of the digital curvelet transform. The algorithm decomposes an n by n image I as a superposition of the form where C_j is a coarse or smooth version of the original image I and W_j represents “the details of I ” at scale J^{-2} , see (Starck et al, 1998) for more information. Thus, the algorithm outputs $J + 1$ subband arrays of size $n \times n$.[The indexing is such that, here, $j = 1$ corresponds to the finest scale(high frequencies).]

For improved visual and numerical results of the digital curvelet transform, presented the following discrete curvelet transform algorithm [5]:

1)Apply the a trous algorithm with J scales

$$I(x,y) = C_J(x,y) + \sum_{j=1}^J W_j(x,y)$$

where c_j is a coarse or smooth version of original image I and w_j represents " the details of I " at scale 2^{-j}

2) set $B_1 = B_{min}$;

3) for $j = 1, \dots, J$ do

a) Partition the subband w_j with a block size B_j and apply the digital ridgelet transform to each block;

The Image Fusion Method Based On The Curvelet The Curvelet Transform

The following is the specific operational procedure for the proposed curvelet-based image fusion approach. while the operational procedure may be generally applied, landsat ETM+ images are utilized as an example in order to illustrate the method.

1) The original Landsat ETM+ panchromatic and multispectral images are geometrically registered to each other.

2) Three new Landsat ETM+ panchromatic images I_1, I_2 and I_3 are produced. The histograms of these images are specified according to the histograms of the multispectral images R, G and B , respectively.

3) Using the well-known wavelet-based image fusion method, we obtain fused images $I_1 + R, I_2 + G$ and $I_3 + B$, respectively.

4) I_1, I_2 and I_3 , which are taken from 2), are decomposed into $J + 1$ subbands, respectively, by applying “a trous” subband filtering algorithm. Each decomposed image includes C_j , which is a coarse or smooth version of the original image, and w_j , which represents “the details of I ” at scale 2^{-j} .

5) Each C_j is replaced by a fused image obtained from 3). For example, (C_j for I_1) is replaced by $(I_1 + R)$.

6) The ridgelet transform is then applied to each block in the decomposed I_1, I_2 and I_3 , respectively.

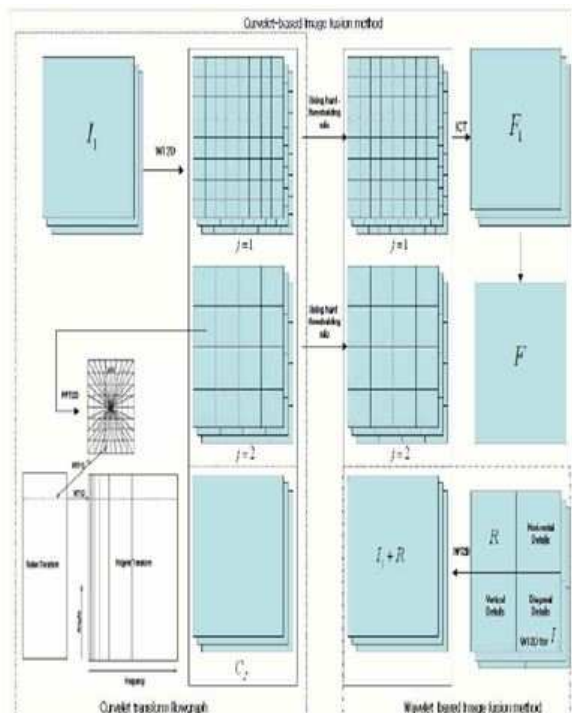


Fig.4. Block diagram image fusion using curvelet transform

7) Curvelet coefficients (or ridgelet coefficients) are modified using hard-thresholding rule in order to enhance edges in the fused image.

8) Inverse curvelet transforms (ICT) are carried out for I1, I2 and I3, respectively. Three new images (F1, F2 and F3) are then obtained, which reflect the spectral information of the original multispectral images R, G and B, and also the spatial information of the panchromatic image.

9) F1, F2 and F3 are combined into a single fused image F.

In this approach, we can obtain an optimum fused image that has richer information in the spatial and spectral domains simultaneously. Therefore, we can easily find small objects in the fused image and separate them. As such, the curvelets-based image fusion method is very efficient for image fusion..

Experimental Study And Analysis

A Visual analysis

Since the wavelet transform preserves the spectral information of the original multispectral images, it has the high spectral resolution in contrast with the IHS-based fusion result, which has some colour distortion. But the wavelet-based fusion result has much less spatial information than that of the IHS-based fusion result.

To overcome this problem, we use the curvelet transform in image fusion. Since the curvelet

transform is well adapted to represent panchromatic image containing edges, the curvelet-based fusion result has both high spatial and spectral resolution

From the curvelet-based fusion result in the Landsat ETM image Fusion presented in Figure 5, it should be noted that both the spatial and the spectral resolutions have been enhanced, in comparison with the original colour image. That is, the fused result contains both the structural details of the higher spatial resolution panchromatic image and the rich spectral information from the multispectral images. Moreover, compared with the fused results obtained by the wavelet and IHS, the curvelet based fusion result has a better visual effect, such as contrast enhancement.

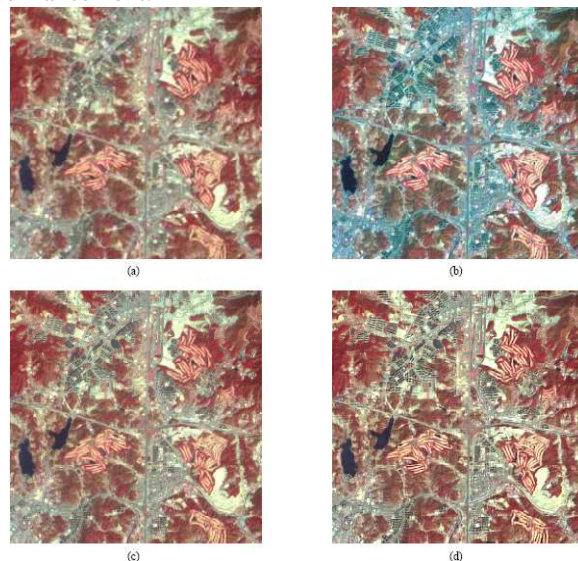


Fig 5.a) Original landsat ETM+ colour image. b) IHS based fusion result. c) wavelet based fusion result. d) Curvelet based fusion result.

B. Quantitative Analysis

In addition to the visual analysis, we conducted a quantitative analysis. The experimental results were analysed based on the combination entropy, the mean gradient, and the correlation coefficient and PSNR. Table I presents a comparison of the experimental results of image fusion using the curvelet-based image fusion method, the wavelet-based image fusion method, and the IHS method in terms of combination entropy, mean gradient, and correlation coefficient PSNR.

In Table I, The mean gradient, the combination entropy, correlation coefficient and PSNR of the curvelet -based image fusion is greater than that of other methods. Thus, the curvelet-based image fusion method is superior to the wavelet and IHS methods in terms of combination entropy.

Method	C. E	M. G	C.C	PSNR
Original Images (R,G,B)	4.4149	14.1035 17.9416 13.3928	- - -	- - -
Image fused by HIS (F1,F2,F3)	7.1287	14.1857 14.9459 14.1517	0. 8134 0. 9585 0. 9303	22.5592 27.9253 23.5900
Image fused by Wavlet (F1,F2,F3)	5.8759	16.5891 18.9083 17.0362	0. 9013 0. 9176 0. 8941	27.7523 25.4509 21.9313
Image fused by Curvelet (F1,F2,F3)	7.4365	19.5549 22.8330 20.9101	0. 9067 0. 9318 0. 9119	25.0602 25.7527 21.2462

TABLE I

A Comparison Of Image Fusion By Wavelet, The Curvelet and His Method

Based on the experimental results obtained from this study, the curvelet-based image fusion method is very efficient for fusing Landsat ETM+ images. This new method has yielded optimum fusion results.

Conclusion

We have presented a newly developed method based on a curvelet transform for fusing Landsat ETM+ images. In this paper, an experimental study was conducted by applying the proposed method, as well as other image fusion methods, to the fusion of Landsat ETM+ images. A comparison of the fused images from the wavelet and IHS method was made. Based on experimental results pertaining to four indicators the combination entropy, the mean gradient, correlation coefficient and the peak signal to noise ratio the proposed method provides better results, both visually and quantitatively, for remote sensing fusion. Since the curvelet transform is well adapted to represent panchromatic images containing edges and the wavelet transform preserves the spectral information of the original multispectral images, the fused image has both high spatial and spectral resolution.

References

[1] T. Ranchin and L. Wald, Fusion of High Spatial and Spectral Resolution images: The ARSIS Concept and Its Implementation,

- Photogrammetric Engineering and Remote Sensing, vol. 66, 2000, pp. 49-61.
- [2] L. Wald, T. Ranchin and M. Mangolini, Fusion of Satellite images of different spatial resolution: Assessing the quality of resulting images," *Photogrammetric Engineering and Remote Sensing*, vol. 63, no. 6, 1997, pp. 691-699.
- [3] J. Nunez, X. Otazu, O. Fors, A. Prades, V. Pala and R. Arbiol, multiresolution-based image fusion with additive wavelet decomposition," *IEEE Transactions on Geoscience and Remote sensing*, vol. 37, no. 3, 1999, pp. 1204-1211.
- [4] E. J. Candès, "Harmonic analysis of neural networks," *A ppl. Comput. Harmon. Anal.*, vol. 6, 1999, pp. 197-218.
- [5] E. J. Candès and D. L. Donoho, Curvelets- A surprisingly effective nonadaptive representation for objects with edges, in *Curve and Surface Fitting: Saint-Malo, A. Cohen, C. Rabut, and L.L. Schumaker, Eds.* Nashville, TN: Vanderbilt University Press, 1999.
- [6] J. L. Starck, E. J. Candès and D. L. Donoho, The curvelet transform for image denoising, *IEEE Trans. Image Processing*, vol. 11, 2002, pp. 670-684.
- [7] J. L. Starck, E. J. Candès, and D. L. Donoho, Gray and Color Image Contrast Enhancement by the Curvelet Transform, *IEEE Trans. Image Processing*, vol. 12, no. 6, 2003, pp. 706-717.
- [8] E. J. Candès, "Ridgelets: Theory and Applications," Ph.D. Thesis, Department of Statistics, Stanford University, Stanford, CA, 1998.
- [9] D. L. Donoho, "Digital ridgelet transform via rectopolar coordinate transform," Stanford Univ., Stanford, CA, Tech. Rep, 1998.
- [10] D. L. Donoho, "Orthonormal ridgelets and linear singularities," *SIAM J. Math. Anal.*, vol. 31, no. 5, 2003, pp. 1062-1099.
- [11] W. Z. Shi, C. Q. Zhu, C. Y. Zhu and X. M. Yang, "Multi-Band Wavelet for Fusing SPOT Panchromatic and Multispectral Images," *Photogrammetric Engineering and Remote Sensing*, vol. 69, no. 5, 2003, pp. 513-520.
- [12] J. B. Sun, J. L. Liu and J. Li, "Multi-source remote sensing image data fusion," *China Journal of Remote Sensing*, vol. 2, no. 1, 1998, pp. 47-50 (in Chinese with abstract in English).